CFD SIMULATION OF HEAT TRANSFER IN A COMPOUND PARABOLIC CONCENTRATOR

By

Niyati A. Vala

14MMEN08

DEPARTMENT OF MECHANICAL ENGINEERING
INSTITUTE OF TECHNOLOGY
NIRMA UNIVERSITY
AHMEDABAD-382 481

MAY 2016

CFD SIMULATION OF HEAT TRANSFER IN A COMPOUND PARABOLIC CONCENTRATOR

Major Project Report

Submitted in Partial Fulfillment of the Requirements for

Semester-IV of

MASTER OF TECHNOLOGY

IN

MECHANICAL ENGINEERING

(ENERGY SYSTEM)

By

Niyati A. Vala

(14MMEN08)

Guided By

Dr. V.J.Lakhera

DEPARTMENT OF MECHANICAL ENGINEERING
INSTITUTE OF TECHNOLOGY
NIRMA UNIVERSITY
AHMEDABAD-382 481
MAY 2016

Declaration

This is to certify that

1. The thesis comprises my original work towards the degree of Master of Technology in Energy System at Nirma University and has not been submitted elsewhere for a degree or diploma.

2. Due acknowledgement has been made in the text to all other material used.

Niyati A. Vala

14MMEN08

Undertaking for Originality of the Work

I, **Niyati A. Vala** , Roll. No. **14MMEN08**, give undertaking that the Major Project entitled "**CFD Simulation of Heat Transfer in a Compound Parabolic Concentrator**" submitted by me, towards the partial fulfillment of the requirements for the degree of Master of Technology in **Mechanical Engineering (Energy System)** of Nirma University, Ahmedabad, is the original work carried out by me and I give assurance that no attempt of plagiarism has been made. I understand that in the event of any similarity found subsequently with any published work or any dissertation work elsewhere; it will result in severe disciplinary action.

Signature of Student

Date:

Place: Nirma University, Ahmedabad.

Endorsed by

(Signature of Guide)

Certificate

This is to certify that the Major Project Report entitled **"CFD Simulation of Heat Transfer in a Compound Parabolic Concentrator"** submitted by **Niyati Vala (14MMEN08)**, towards the partial fulfillment of the requirements for the award of Degree of **Master of Technology in Mechanical Engineering (Energy System)** of Institute of Technology, Nirma University, Ahmadabad is the record of work carried out by her under our supervision and guidance. In our opinion, the submitted work has reached a level required for being accepted for examination.The result embodied in this major project, to the best of our knowledge, has not been submitted to any other University or Institution for award of any degree.

Dr. V. J. Lakhera
Guide and Professor,
Department of Mechanical Engineering,
Institute of Technology,
Nirma University,
Ahmedabad.

Dr. R. N. Patel
Head of Department,
Department of Mechanical Engineering,
Institute of Technology,
Nirma University,
Ahmedabad.

Dr. P. N. Tekwani
Director
Institute of Technology,
Nirma University,
Ahmedabad.

Acknowledgments

With great pride and pleasure, I express my sincere gratitude to my project guide **Dr. V. J. Lakhera** for helping me with the conceptualization of the idea for the project, providing the technical assistance and prompt suggestions from them during my thesis work. I am also thankful to Prof. Leena Bora for their valuable suggestion and conceptual clarity of the topic in detail that helped me a lot during this work.

I would like to thank **Dr. R. N. Patel** Head of Mechanical Engineering Department, for having faith in me and supporting me throughout my endeavor.

I am very much thankful to **Dr. P. N. Tekwani** (Director , IT, NU) who have directly or indirectly helped me during this dissertation work.

I am also thankful to all faculty members of Department of Mechanical Engineering, Nirma University,Ahmedabad for their special attention and suggestion for work.

The blessing of God and my family made the way for this dissertation work. I am very much grateful to them.

The friends, who always bear and motivated me throughout my thesis work, I am thankful to them

Abstract

Concentrating collectors are applicable where the temperature requirement are of 100^{o}C or above. Compound Parabolic Concentrator (CPC) is a special type of solar collector fabricated in the shape of two meeting parabolas and is among the collectors having the highest possible concentration ratio. Also because of its large aperture area, only intermittent tracking is required. It is mostly used in industrial applications where medium pressure steam is required (at around 150°C). In order to investigate the heat transfer in a Compound Parabolic Concentrator, it is important to understand the influence of Concentration Ratio (CR) and surface radiation properties of the collector surface. With these objectives, a model was developed in CREO software and was analyzed by Computational Fluid Dynamics (CFD) technique using ANSYS Fluent and the influence of Concentration Ratio (CR of 1, 2 and 3) and surface radiation properties of the collector surface on the temperature distribution within the CPC was studied. The CFD analysis considering different concentration ratio and surface properties (radiation related) reveal that the highest tube surface temperature are obtained for a concentration ratio of 3 with tube surface emissivity of 0.9 and reflector surface reflectivity of 0.9.

Contents

Declaration ii

Undertaking iii

Certificate iv

Acknowledgments v

Abstract vi

Table of Contents vii

List of Figures viii

List of Table ix

Abbriviations x

1 Introduction 1

1.1 Solar Concentrators 1

1.2 Different Types of Solar Concentrators 1

1.2.1 Parabolic Concentrators 2

1.2.2 Hyperboloid Concentrators 2

1.2.3 Fresnel Concentrators 2

1.2.4 Compound Parabolic Concentrators 3

1.2.5 Dielectric Totally Internally Reflecting Concentrators 3

1.2.6 Flat High Concentration Devices 3

1.2.7 Quantum Dot Concentrators 3

1.3 Compound Parabolic Concentrators 3

1.3.1 Basic Theory of CPC 3

1.3.2 Description of CPC 4

1.3.3 Advantages and Disadvantages 7

1.3.4 Construction and Working of CPC 8

1.3.5 Generation of the Geometry of CPC 9
1.3.5.1 For Concentration ratio 1: 9
1.3.5.2 For Concentration ratio 2: 9
1.3.5.3 For Concentration ratio 3: 9
1.3.6 Comparisons with other Concentrating Collectors 11
1.4 Motivation for Present Study 11
1.5 Objective of Present Study 12
1.6 Outline of the Project 12

2 Literature Review **13**
2.1 General 13
2.1.1 Schematic Design of CPC 15
2.1.2 Different Shape of Absorbers 16
2.2 Testing on CPC 16
2.2.1 Preliminary diagnostic testing 16
2.2.2 Optical testing 16
2.2.3 Performance testing 17
2.3 Computational Domain 17
2.4 Summary of Literature Reviewed 18

3 Computational Fluid Dynamics Analysis of CPC **21**
3.1 CPC Geometry Model Description 21
3.1.1 Numerical model of CPC 21
3.2 Computational Procedure in FLUENT ANSYS (Mesh generation) 22
3.2.1 Setup for Simulation Analysis 22
3.2.2 Mesh Report of Geometry 25
3.2.3 Solution Method of CPC 25
3.3 Boundry conditions for CFD simulation of CPC 27
3.3.1 Boundary Conditions in CFD analysis for Concentration Ratio 1: . 27
3.3.2 Boundary Conditions in CFD analysis for Concentration Ratio 2: . 28
3.3.3 Boundary Conditions in CFD analysis for Concentration Ratio 3: . 29
3.4 Governing Equations used in simulation 29
3.4.1 Mass conservation (Countinuity) Equation: 29
3.4.2 Momentum Conservation Equation: 29
3.4.3 Energy Conservation Equation: 30
3.4.4 Radiation Equation 30

4 Results and Discussion **31**
4.1 Temperature distribution in CPC for CR-1 31
4.2 Temperature distribution in CPC for CR-2 32

4.3 Temperature distribution in CPC for CR=3 34
4.4 Discussion 36

5 Conclusion and Future Work **38**

List of Figures

1.1 Cross section of CPC [5] 5
1.2 Fabricated Compound Parabolic Concentrator [5] 6
1.3 Construction of a Compound Parabolic Concentrator [5] 8
1.4 Model of CPC (with concentration ratio 1) using CREO 10
1.5 Model of CPC (with concentration ratio 2) using CREO 10
1.6 Model of CPC (with concentration ratio 3) using CREO 11

2.1 Reflector coupled to Tubular Nonevocueted Receiver [2] 15
2.2 Different Shape of Absorbers [13] 16

3.1 Detail of mesh 3D-A showing the area around the absorber tube 23
3.2 Meshing of geometry (CR-1) 24
3.3 Meshing of geometry (CR-2) 24
3.4 Meshing of Geometry (CR-3) 25
3.5 Boundary Condition for CR-1 27
3.6 Boundary Conditions for CR-2 28
3.7 Boundary Condition for CR-3 29

4.1 CR-1 : Maximum mean Temperature at middle plane 32
4.2 CR-1 :Temperature of tube surface 32
4.3 CR-2: Maximum mean Temperature at middle plane 33
4.4 CR-2: Temperature of tube surface 34
4.5 CR-3 :Maximum mean Temperature at middle plane 35
4.6 CR-3:Temperature of tube surface 35

List of Tables

2.1 Papers for References 20

3.1 Mesh report of geometry 25

4.1 Results of CR-1 31
4.2 Results of CR-2 33
4.3 Results of CR-3 34
4.4 The avarage temperature of tube surface for various CR and surface characteristics 36
4.5 The mean fluid temperature at middle plane for various CR and surface characteristics 37

Abbreviations

a	Annum
A	Area (m^2)
C	Optical Concentration, $C = A_{ape} / A_{abs}$
C_c	Collector Capacity (kJ/K)
C_p	Specific Fluid Capacity (kJ/kg K)
I	Solar Radiation (W/m^2)
F'	Absorber Efficiency Factor
IAM	Incidence Angle Modifier
K	Ray Loss Factor
m	Mass (kg)
t	Time (s)
T	Temperature (^0C)
p	Pressure (Pa)
ϑ	Incidence Angle (^{0})
α	Slope (^{0})
β	Azimuth Angle (^{0})

Subscripts

A	Acceptance
ape	Aperture
abs	Absorber
amb	Ambient
dir	Direct
gla	Glass
los	Losses
ref	Reflector
tot	Total

Greek

α	Absorption
ε	Emission
η	Optical Efficiency Factor
ρ	Reflexion
σ	Stress
τ	Transmission

Chapter 1

Introduction

1.1 Solar Concentrators

Huge amount of energy is available in the core of sun. Solar concentrator is the device which is used to collect the heat from the sun in the form of radiation and transfer this collected heat to the fluid passing in contact with it. They are classified into two main types: (1) Flat plate collectors (2) Concentrating Collectors. Each concentrating collectors are separated into two groups: (a) Focusing or Imaging type (b) Non-focusing or non-imaging type.

Compound parabolic concentrator is defined as under, it is one of the non-imaging type concentrating solar concentrators. It consists of two parabolic reflectors at the two ends of the absorber plate and hence it is known as compound parabolic concentrator.

Solar concentrator permits the collection of sunlight from a large area, and then focusing it on a smaller receiver or exit of the device. To generate the electricity the concept wise representation of a solar collector used in harnessing the power from the sun.

The usage decide which type of material is used to fabricate the concentrator. Most of the collectors are made from mirrors while for the BIPV system, for solar thermal. The material which is used for concentrator is made from glasses or transparent plastic. As these materials are very cheap as compared to the PV material. The cost per unit area of a PV material is costlier than the price per unit area of a solar concentrators. By introducing this concentrator, not only the total cost of the solar cell could also be reduced but exact amount of energy could be collected from the sun. It has been concluded that the almost all cost-effective PV for commercial application in the future will be dominated by high concentration collector which is incorporated by high-efficiency cell.

1.2 Different Types of Solar Concentrators

The various type of solar concentrators developed in the past four decades include:

- Parabolic Concentrator
- Hyperboloid Concentrator
- Fresnel Lens Concentrator
- Compound Parabolic Concentrator (CPC)
- Dielectric Totally Internally Reflecting Concentrator (DTIRC)
- Flat High Concentration Devices
- Quantum Dot Concentrator (QDC)

1.2.1 Parabolic Concentrators

A parabola equals to the two dimensional design of a parabolic concentrator. Parabolic Concentrators are used in so many places like a reflecting solar concentrator. A different property of the concentrator is that it can focus all the parallel rays from the sun and it collect it to a single focus point. The whole part of the parabola curve is not compulsory to construct the concentrator. Maximum of the parabolic concentrator focuses only a truncated portion of the parabola of the collector.

1.2.2 Hyperboloid Concentrators

The Hyperboloid Concentrator design consists of two hyperbolic section. It can be produced by rotating the two dimensional design with its symmetrical axis. Whether the inside wall of the hyperbolic profile is considered as a mirror, the sun rays entering the concentrator will be reflected and it will be focused to the exit aperture.

1.2.3 Fresnel Concentrators

Fresnel lens react same as how the conventional lens reacts. If we refract the rays and focusing them at one focal point.it gives more accurate results. Fresnel Collector has two section (1) The flat upper surface (2) The back surface. Which employs canted facets. The angle is made from an approximation of the curvature of a lens which is used in geometry. There are two ways to use this concentrator (1) Point focus Fresnel lens (2) Line focus Fresnel lens.

Fresnel lens is better than a conventional lens because it is leaner and requires a lesser amount of fabrication material. This type of Concentrator has the capability to separate the direct the light and diffuse the light. Due to the sharpness this concentrator will be not beneficial. The manufacturing process's error could create a circle shape at the edges of the facets. That causing the rays improperly focused at the receiver.

1.2.4 Compound Parabolic Concentrators

The full length of a CPC depends both on the exit aperture and the acceptance angle of the concentrator, If the acceptance angle reduced, the size of the concentrator will be increased. The CPC is used as a three dimensional rotational symmetry concentrator and it is also used same as a CPC trough concentrator. After designing of the CPC, It is normally employed as a reflector in a solar power plant.

1.2.5 Dielectric Totally Internally Reflecting Concentrators

The two ways are used to product the DTIRC. First one is maximum concentration method and second one is phase conserving method. Both the methods will create relative identical structure. Among the two the first technique offers slightly higher concentration so it is more suitable for solar application. DTIRC consists the three parts (1) Curved front surface (2) totally internally reflecting side profile and last one is (3)exit aperture., When they are refracted and directed to the side profile, the rays hit the front curved surface. They will be totally internally reflected to the exit aperture after hitting the sidewall.

1.2.6 Flat High Concentration Devices

The concentrators which are capable to achieve theoretical maximum acceptance-angle-concentration is known as Flat High Concentrators. Flat High concentrators have two biggish benefits, which are as under, first one is they are very compact and second one is that they offer very high concentration. It is difficult to create electrical connection and heat sinking, However the disadvantages of this design is negligible. Due to the cell's position.

1.2.7 Quantum Dot Concentrators

The planar device consists of three parts(1) A transparent sheet of glass or plastic made doped with quantum dots (QDs) (2) Reflective mirrors mounted on the three edges and back surface, and (3) An outlet where a PV cell is attached is called as Quantum dot concentrator (QDC) .

1.3 Compound Parabolic Concentrators

1.3.1 Basic Theory of CPC

Compound parabolic concentrator is defined as one of the non-imaging type concentrating solar collector. CPC consist of two parabolic reflectors at the two ends (left and right).

It has an absorber plate and therefore it is known as compound parabolic concentrator.

1.3.2 Description of CPC

CPC has three elements in it's geometry

1. **Receiver**: The largest absorbance for solar radiation is in the receiver as possible and must be constructed with high-conductivity metals, work efficiently the absorbed heat into the heat transfer fluid. Most receiver materials do not have a very high absorb radiation, and they need to be quotation of special covered which has special solar selective surface coatings [3]. Solar energy made from a silicon polymer, with an emissivity from 0.28 to 0.49 and absorbance values from 0.88 to 0.94 was applied upon the surface of this receiver which is used in commercial selective surface.

2. **Cover**: The cover is made up from a transparent insulation that allows the passage of solar radiation to reflector and receiver, and a low transmittance of the thermal radiation from the receiver that having a high transmittance of solar radiation, It must have the high durability and low cost.

3. **Reflector**: Solar concentrators having the largest reflectance among all parts. It focuses beam-solar radiation onto the receiver, and it is located at the focus of CPC. For best performance of CPC, each material component was alertly selected. The general Concentration Ratio for a CPC is around 3 –10.

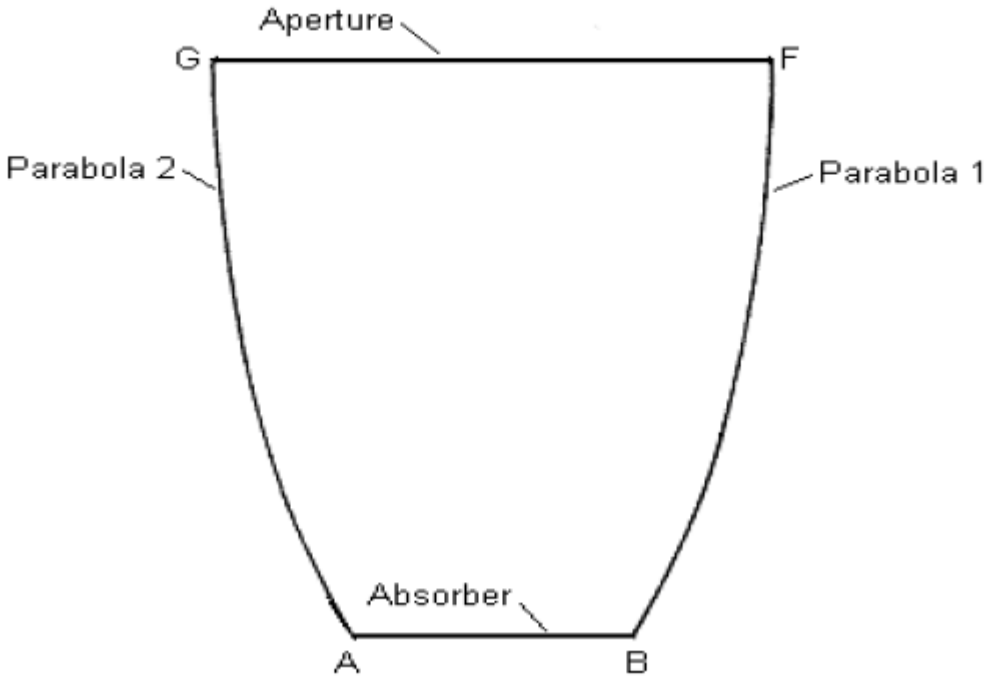

Figure 1.1: Cross section of CPC [5]

Aperture Area = W* L
Absorber Area = b * L
Concentration Ratio C = W/b
The maximum possible concentration for a given acceptance half angle to be
Concentration ratio, C=1/sinϑ
(by the the Second Law of Thermodynamics)

Figure 1.2: Fabricated Compound Parabolic Concentrator [5]

There are some of the terms that are present when discussing Concentrating Collectors [2]

1. **Aperture Area (A_a)**: It is the plane opening of the concentrator through which the incident solar flux is accepted. For a cylindrical or linear concentrator it is characterized by the width, as for a surface of revolution it is characterized by the diameter of opening.

2. **Absorber Area (A_{abs})**: It is the total area receiving the concentrated radiation. It is also the area from which useful energy is delivered from the system.

3. **Acceptance Angle ($2\vartheta c$):** It is limiting angle over which incident ray path may deviate from normal to the aperture plane and still field the absorber. Concentrators with large acceptance angle need to be moved on seasonally while concentrators with little acceptance angle need to be moved continuously to track the sun.

4. **Geometric Concentrating Ratio (C)**: It is the ratio of effective area of the aperture to surface area of the absorber. Value of concentrating ratio varies from (limiting value for a flat plate collector) few thousand (for a paraboloid collector). C = Aa / Aabs.

5. **Local Concentration Ratio**: It may so happen that absorber in some systems may not be fully or uniformly illuminated, thus in order to characterize this local concentration this term is defined. It is defined as ration of flux arriving at any point on the absorber to the incident flux at the entrance aperture of the concentrating system.

6. **Intercept Factor (Y)**: It is the fraction of focused energy intercepted by the absorber of a given size. As a typical concentrator receiver design its value depends on the size of absorber, generally is has a value greater than 0.9.

7. **Collector (Thermal) Efficiency (η_c)**: It is the ratio of useful energy delivered to the absorber to the energy incident on the aperture. ηc = qu / Ib qu is the rate of useful energy per unit aperture area and Ib is the incident solar energy.

8. **Optical Efficiency (η_o):** It is defined as the ratio of the energy absorbed by the absorber to that incident on collector. It includes the effect of mirror surface, shape, transmission losses, tracking accuracy, shading by receiver, absorption and reflection properties, solar beam incident angle. ηo = qu / ($\alpha\tau$Ib) qu is the rate of useful energy per unit aperture area Ib is the incident solar energy and α, τ are the function of angle of incidence of radiation on the aperture Uc, is the heat loss coefficient based on receiver area, Ta and Tc are the ambient temperatu•re and collector temperature The concentration ratio is limited as the sun of finite size, determined by the shape factor; the concentration ratio for 2-D collector like cylindrical parabolic collector is limited by the value 1 /sin ϑmax .

1.3.3 Advantages and Disadvantages

The biggish advantages of CPC are that, it can receive radiation radiation arriving with large angular spread and yet concentrate it on to linear receivers of small transverse width. The incident rays after reflection from the reflector are not focused at a point, but are simply collected on absorber surface.

1. In solar still plant – to remove impurity and microbes from the water

2. solar water heating – in buildings used for domestic water heating purpose.

3. In power generation –photovoltaic cells

4. for solar cooking

Tracking of a CPC as discussed earlier may not be required If CPC has concentration ratio of 3 – 5, and high acceptance angle. CPC is generally oriented in the East – West direction with south facing aperture area, so that the maximum sunlight is utilized. However for

application where concentration ratio is very high or the acceptance angle is less, than tracking is to be provided to ensure that sunlight falls continuously on CPC.

The CPC should be used in great variety of solar applications such as passive (integrated collector storage) and active (direct and indirect circulation) solar water heating, space heating and hot water production, heat pumps, sorption cooling and refrigeration systems, industrial air and water systems to process heat; desalination (multistage flash, multiple effect boiling, vapor compression), and solar chemical systems for thermal power systems.

1.3.4 Construction and Working of CPC

The geometry of a CPC is shown in Fig1.3 . It's having two parabola sections AB and CD of parabola 1 and 2 respectively. AD is the aperture area with width W, and BC is the absorber area with width b. the axis are oriented in such a way that C is the focus of parabola 1 and B is the focus of parabola 2 which is shown in figure. Also the height of the collector is decided that tangents at A and D are parallel to the axis of the collector.

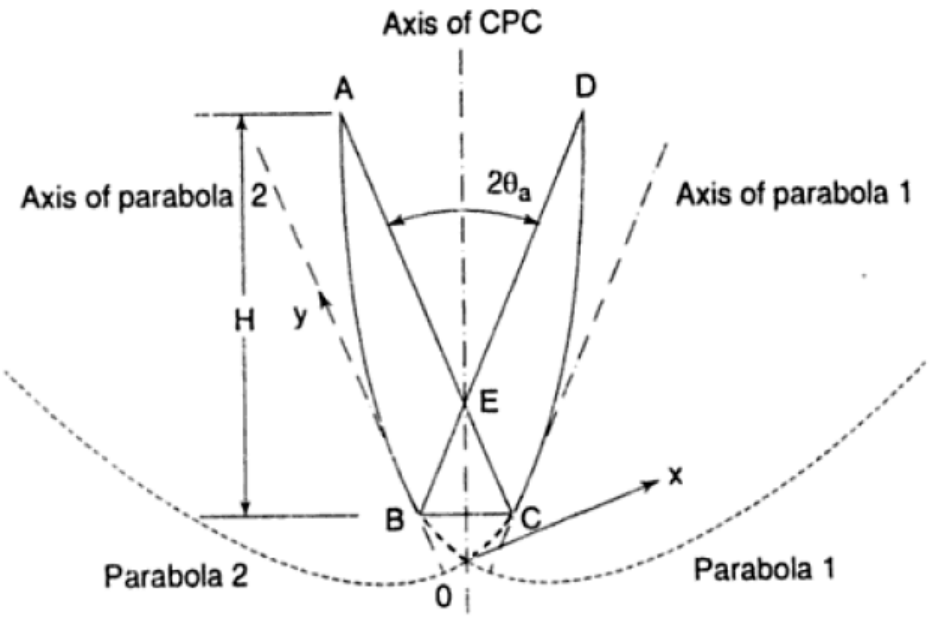

Figure 1.3: Construction of a Compound Parabolic Concentrator [5]

The acceptance angle of CPC is the angle AED. It is obtained by joining a focus to the opposite aperture edge. Concentration ratio is given by w/b. The calculations of Height and aperture area for the CPC as per the desired operating temperature. Height is generally truncated to half as it doesn't much affect the concentration ratio to reduce the cost. Acceptance angle is also generally kept large so that tracking may be required intermittent only. Optical efficiency for CPC is around 65%, which is 8% more as compared to a

parabolic trough collector. The amount of diffused radiation that can be collected is given by 1 /CR (concentration ratio) for a concentrating collector. The general Concentration Ratio (CR) for a CPC is around 3 –10, while that for PTC and Parabolic Dish Collector is more than 1000. So the advantage of a CPC is that it can collect diffuse radiation too. So it is benificial in cloudy atmosphere too.

1.3.5 Generation of the Geometry of CPC

Here the reflector profile is designed and fabricated for a half acceptance angle and a spherical copper absorber of radius (r). For obtaining the profile of the parabola the following equations suggested by Rabl [1] are used.

$x = r \sin\vartheta - \rho \cos\vartheta$ ..... (1)

$y = - r \cos\vartheta - \rho \sin\vartheta$ ..... (2)

Where, $\rho = r\,\vartheta$ for $\vartheta \leq \vartheta 1$

$\rho = (\vartheta + \vartheta a + \pi/2 - (\cos(\vartheta - \vartheta a))) \,/\, (\,1 - \sin(\vartheta - \vartheta a))$

for $\vartheta 1 < \vartheta \leq \vartheta 2$ and $\vartheta 1 = \vartheta a + \pi/2$; $\vartheta 2 = 3\pi/2 - \vartheta a$

1.3.5.1 For Concentration ratio 1:

For $\vartheta a = 90°$ ϑ(initial) = 45° and ϑ(last) = 180°, by taking the value of ϑ = 45° to 180°, in the intervals of 10°, the values of x and y are calculated using equations (1) and (2). Using the values of x and y, a smooth curve is drawn (which gives the right half of the parabola) as shown in Fig 1.3. The mirror image gives the left half, that result in two-dimensional view of the 3-D CPC. Rabl [4] pointed out that top portion of reflector area can be truncated without significantly reducing concentration.

1.3.5.2 For Concentration ratio 2:

For $\vartheta a = 30°$ ϑ(initial) = 15° and ϑ(last) = 255°, by taking the value of ϑ = 15° to 255°, in the intervals of 10°, the values of x and y are calculated using equations (1) and (2). Using the values of x and y, a smooth curve is drawn (which gives the right half of the parabola) as shown in Fig 1.3. The mirror image gives the left half, that result in two-dimensional view of the 3-D CPC. Rabl [4] pointed out that top portion of reflector area can be truncated without significantly reducing concentration.

1.3.5.3 For Concentration ratio 3:

For $\vartheta a = 20°$ ϑ(initial) = 10° and ϑ(last) = 250°, by taking the value of ϑ = 10° to 250°, in the intervals of 10°, the values of x and y are calculated using equations (1) and (2). Using the values of x and y, a smooth curve is drawn (which gives the right half of the

parabola) as shown in Fig 1.3. The mirror image gives the left half, that result in two-dimensional view of the 3-D CPC. Rabl [4] pointed out that top portion of reflector area can be truncated without significantly reducing concentration.

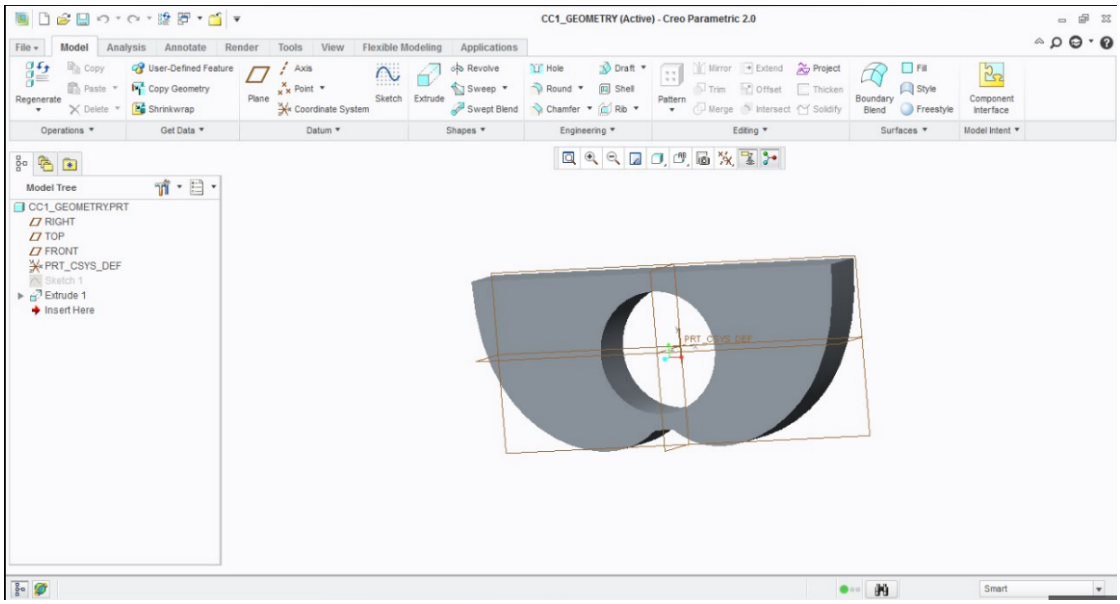

Figure 1.4: Model of CPC (with concentration ratio 1) using CREO

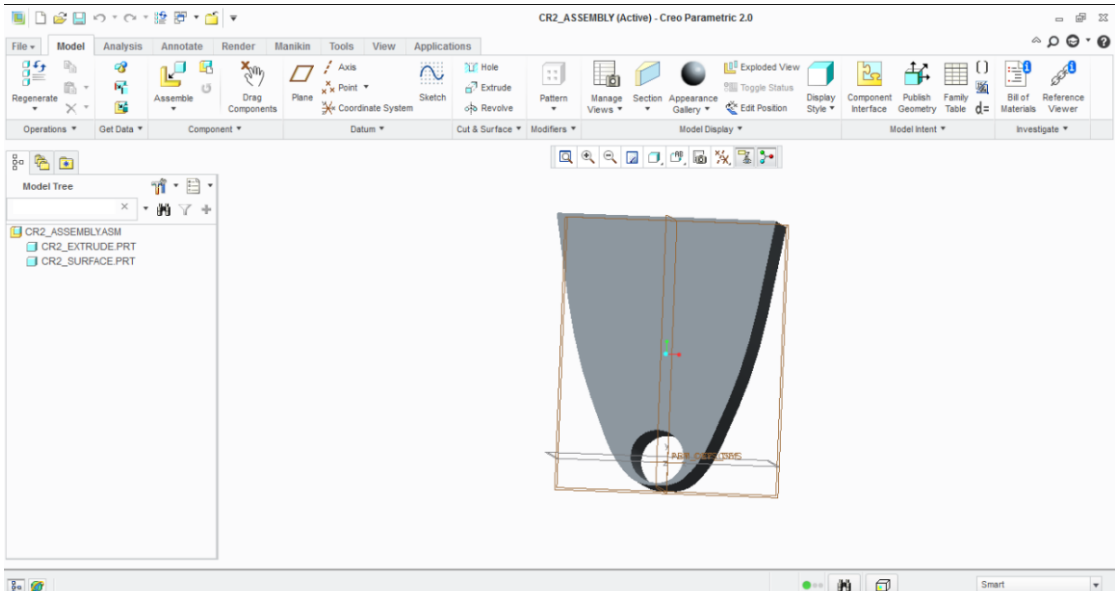

Figure 1.5: Model of CPC (with concentration ratio 2) using CREO

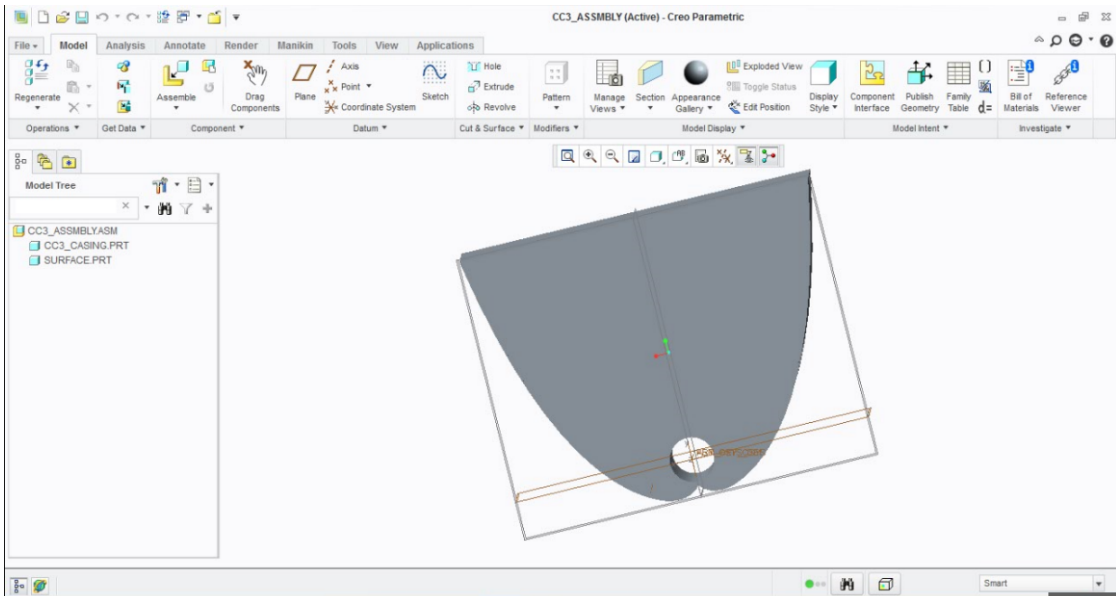

Figure 1.6: Model of CPC (with concentration ratio 3) using CREO

1.3.6 Comparisons with other Concentrating Collectors

1. CPC can concentrate diffused radiation, other concentrating collectors as parabolic dish and PTC only concentrates beam radiation component on the solar radiation. Component of diffused radiation that can be collected is given by 1 / CR. As the concentration ratio for CPC is smaller, it can concentrate diffused radiation.

2. Mostly the CPC are of larger acceptance angle and are oriented in the east west direction. So only intermittent tracking every 15 days or even up to every 2 months (for concentration ratio 3 – 5) is needed. A continuous tracking is required for the best performances of parabolic trough and parabolic dish collectors.

3. Parabolic dish collector can save temperature up to 500°C

4. As compared to other concentrating collectors, CPC are economical.

1.4 Motivation for Present Study

- The CPC or Compound Parabolic Collector can be effectively used as a low cost solar collector technology for various applications at moderate temperature above 100·C. The CPC has the advantage of an ease of fabrication, no need for continuous tracking and simpler support structure. The motivation for the present study is to understand the temperature profile in a CPC for various concentration ratio and surface charactristics.

1.5 Objective of Present Study

The objective of the present study include:

1. To model a CPC for further thermal analysis
2. To predict the temperature profile within the CPC for understanding the influence of Concentration ratio and surface (radiation) charactristics on the CPC performance.

1.6 Outline of the Project

The report consists of five chapters. The first chapter deals with introduction, objective and methodology of my work. In the second chapter, detail description of literature is shown for review. The third chapter presents, mesh generation and CFD analysis of the geometry. Results and Discussion is presented in fourth chapter. Conclusion is concluded in Fifth chapter. References are marked in last.

Chapter 2

Literature Review

2.1 General

In various situations, in particular in solar energy applications, the following problem arises: how can radiation, which is diffusely distributed over a range of angles 0' with |0'1-< 0, and incident on an aperture of area AL, be concentrated onto a smaller absorber area As, and what is the highest possible value of the concentration C = AL/As ? Winston [6] has analyzed this problem from first principles and found an elegant solution. Using the principle of phase space conservation, he proved that the ideal limit is

$C_{ideal} = \frac{A_L}{A_S} = \frac{n}{sin\theta}$

where n is the index of refraction of the medium surrounding the absorber. (For a simple derivation of this result directly from the 2nd law of thermodynamics, Rabl [2]). He also found a class of non-imaging instruments, so called compound parabolic concentrators, henceforth referred to as CPC, which actually achieve this ideal performance; imaging instruments such as Fresnel lenses or simple parabolic mirrors fall short of this value by at least a factor of two [3].

Recently, Winston proposed the use of the CPC principle for solar energy collection. The CPC is well suited for this application because it guarantees the highest possible concentration for any angular acceptance [6].

Computationally much cheaper Steady calculations, lead to a reasonable overall agreement of velocity field. After performing the analysis the temperatures recorded at the mirror and the glass cover are well matched. The resolution of the mesh is good enough to allow heat conduction even in thin features of the geometry (mirror and tube). From this knowledge we studied several scenarios, which are important for applications like

- Reduced air pressure
- Inert gas fillings
- Temperature dependent material parameters or [2]

At last, from these simulations, we demonstrate the level of detail, which can be obtained. It can be separated the individual heat transfer mechanisms like conduction, convection and radiation and to quantify their contributions to heat loss of the collector.

Along the axis of the two parabolas Conventional solar compound parabolic concentrators are normally fitted with one tubular receiver position. This work investigates the potential of using either two tubular receivers in an elliptical single receiver or one compound parabolic concentrator.

The optical efficiency of a compound parabolic concentrator with two tubular receivers aligned horizontally and vertically was predicted, by using advanced ray tracing technique.After experiment results showed that the horizontal configuration of performance both the vertical and the single configurations by up to 15%. Also, a horizontally aligned elliptical single tube showed an increase in the average daily optical efficiency by 17% compared to the single tube configuration.

At different acceptance angles, The thermal performance of the single and double horizontally aligned tubular receivers was determined from the optical simulation using the thermos syphon heat pipe experimentally tested utilizing the heat flux obtained. After performing the experiments we concluded that double tube configuration thermally shows the single one heat transferred to the water cooling by 21%, 19.8% and 18.3% for acceptance angles of 10°c, 20°c and 40°c respectively. The work shows the ability of using single elliptical or two tubular receivers one aligned horizontally in one concentrator to improve the optical and thermal efficiencies of compound parabolic collectors [11]

Because of the achievement of the highest possible concentration for any acceptance angle, Compound Parabolic Concentrators (CPC) are relevant for solar energy collection (tracking requirement). The convective and radiative heat transfers through a CPC are calculated, and formulas for evaluating the performance of solar collectors based on the CPC principle are presented [11]. For computing optical losses, a simple analytic technique for counting the average number of reflections for radiation passing through a CPC is developed; this is useful In most practical applications, a CPC will be truncated because a large portion of the reflector area can be eliminated without seriously reducing the concentration . The effects of this truncation are described explicitly. The paper includes many numerical examples, displayed in tables and graphs, which should be helpful in designing CPC solar collectors [2].

2.1.1 Schematic Design of CPC

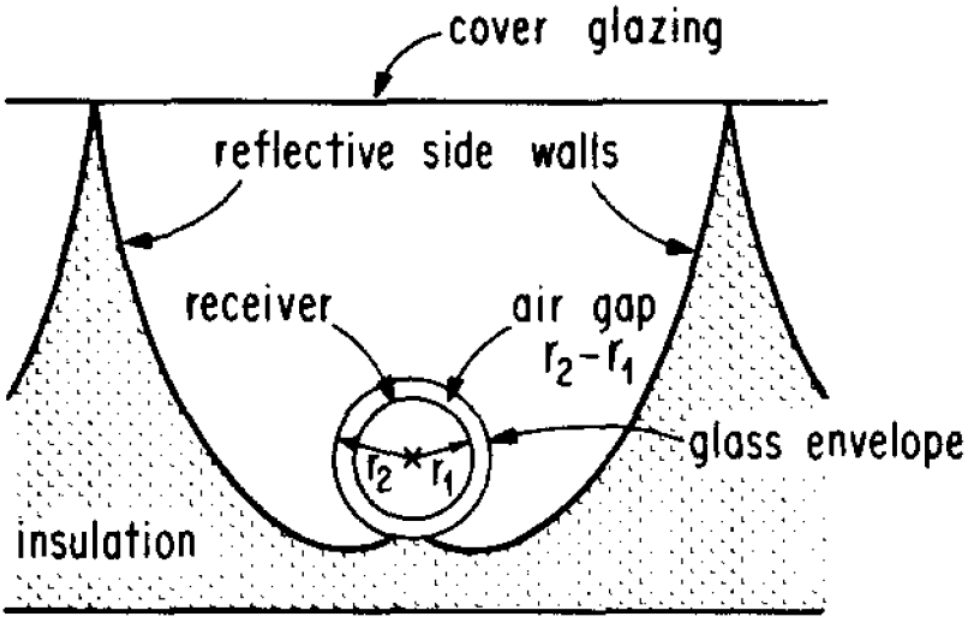

Figure 2.1: Reflector coupled to Tubular Nonevocueted Receiver [2]

Schematic design for a "double glazed" non-evacuated CPC in which the absorber tube is enclosed in a glass tubular convective barrier. Such a design would be practical with low cost antireftective coatings and highly reflective mirrors.

The heat loss can be calculated by the methods of Ref. [7]. Choosing the width of the air layer between absorber and inner surface of the glass envelope involves a compromise because for a small gap conduction is large whereas a large gap implies high optical losses.

In particular we found that the angular acceptance properties, on which the seasonal tilt schedule depends, agreed very well with nominal design values. With conventional reflectors the optical efficiencies are somewhat lower than for flat plate collectors. Inexpensive reflector materials (i.e. aluminized plastic reflectors or aluminized films on a thin substrate) could be used.

2.1.2 Different Shape of Absorbers

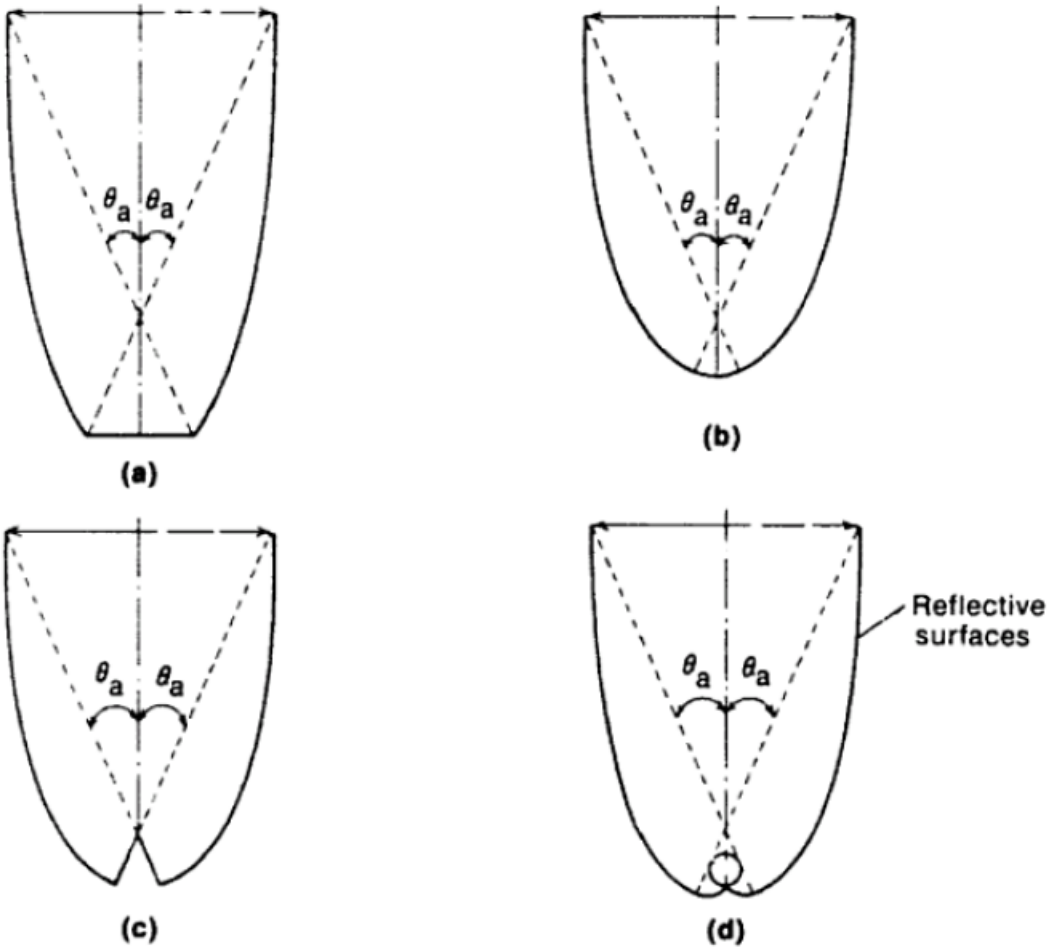

Figure 2.2: Different Shape of Absorbers [13]

2.2 Testing on CPC

2.2.1 Preliminary diagnostic testing

For this purpose a single trough prototype module consisting only of the absorber fin and CPC reflector was built. The reflector was fastened to wooden ribs and mounted within a plywood box with an acrylic glazing. In this diagnostic test module, in contrast to the prototype module actually performance tested, no insulation was used behind the reflector other than the dead air space between the reflector sheets and the plywood box [3]

2.2.2 Optical testing

The visual inspection method was applied only to evaluate the quality of the mirror contour by making sure there were no reflecting shiny patches when the aperture was

viewed from a distance. A quantitative visual measure of the acceptance angle was not carried out.

2.2.3 Performance testing

The optical and thermal performance of the full two trough module was measured using the same procedures as used for the original collector and unfortunately did not utilize some of the refinements and standardization procedures which we developed at a later time.

2.3 Computational Domain

The subsequent analysis of the temperature distribution in the collector has been performed using the computationally cheap 3D transient simulations, because it is sufficient to reproduce the main features to achieve reasonable overall agreement of the temperatures. These points are close to the recirculation zone, where the 3D-steady simulations do not resemble the experimental flow pattern. 3D calculations reproduce the temperature behavior sufficiently well. There are several important aspects: The mesh resolution of the absorber tube and mirror thickness is critical and can lead to large temperature variations. This is especially true when modelling the mirror only as an infinitesimal thin wall. In this case the heat flow is forced normal to the mirror wall, which inhibits a redistribution of the temperature along the mirror. This condition creates strong local variations in temperature, leading to large deviations in the mirror temperature of up to 20 C compared to the experiment. The other meshes, which resolve the thickness and allow thermal redistribution along the mirror, closely resemble the experimental data with very similar results for a resolution of one, three and five cells. The total heat loss (convective and radiative) of the absorber to ambient is affected in the following way: If the absorber and mirror thickness is not resolved, the heat transfer is reduced by 10% in the reference case compared to mesh (CR-1) with the best resolution. (This would over predict the performance of the collector in efficiency calculations.) The total heat transfer for the other meshes (CR-2 and CR-3) only differ by 1% compared to the results of mesh CR-1. This agrees with the results of the temperature distribution and shows again that the number of cells in the mirror and tube is not critical as long as the thickness is resolved. When introducing the heat source terms on the absorber to model incoming irradiation, the temperature on the tube and its redistribution will also be important due to the focusing of the CPC [8]

2.4 Summary of Literature Reviewed

Author	Field	Title	Highlights
Ch. Reichl, F. Hengstberger, Ch. Zauner.	Elsevier-solar energy	Heat transfer mechanism in a compound parabolic concentrator. Comparison of computational fluid dynamics simulation to partical image velocimetry and local temperature measurement	• Particle image velocimetry (PIV) and local temperature measurements have been carried out on a lab scale compound parabolic concentrator (CPC) collector model various absorber temperatures and tilt angles. • The results of these experiments are compared to computational fluid dynamics (CFD) calculations of the velocity field and temperature distribution. • It will be founded that transient simulations in 3D are required for a detailed reproduction of the natural convection currents obtained by PIV. Steady calculations in 2D, which are computationally much cheaper, lead to a reasonable overall agreement of the velocity field
A.A. Hachicha, I. Rodriguez, R. Capdevila, A. Oliva	Applied Energy	Heat transfer analysis and numerical simulation of a parabolic trough solar collector	• Heat transfer analysis of a heat collector element is proposed • The circumferential distribution of the solar flux around the receiver is studied.
A.A. Hachicha, I. Rodríguez, O. Lehmkuhl, A. Oliva	Energy Procedia	On the CFD & HT of the flow around a parabolic trough solar collector under real working conditions	• A wind flow analysis around a parabolic trough solar collector under real working conditions is performed. • A numerical aerodynamic and heat transfer study based on Large Eddy Simulations is carried out to characterize the

Author	**Field**	**Title**	**Highlights**
Frank Buttinger, Thomas Beikircher, Markus Proll, Wolfgang Scholkopf	Solar Energy	Development of a new flat stationary evacuated CPC collector for process heat applications.	• For the economical supply of a solar process heat at temperatures between 120 and 150 a new non tracking, flat, low concentarting collector has been developed. • The new collector is an edge ray collector with a concentration of 1.8 and inert gas filling, existing of parallel mounted absorber-reflector units, aligned in east-west directions. • To suppress heat losses due to gas convection inside, air or inert gas like krypton at a pressure below 10 mbar is used.
Pedro Horta, J.C.C. Henriques, Manuel Collares-Pereira	Solar Energy	Impact of different internal convection control strategies in a non evacuated CPC collector performance.	• Over last many years ago the technological features observed in solar concentrator materials, namely better selective absorber coatings and very clear glass covers, help to performance improvement and translate into higher operational temperature ranges with higher efficiency values.
ARI Rabl	Solar Energy group	Optical and Thermal Properties of Compound Parabolic Concentrator	• Compound Parabolic Concentrators are relevant for solar energy collection because of achievement of of highest possible concentration for any acceptance angle • It will be analyzed the radiative, convective and conductive heat transfermodes in solar collectors related on collector's principle.

Author	Field	Title	Highlights
B. Abdullahi, R.K. AL-Dadah, S. Mahmoud, R. Hood	Applied Energy	Optical and thermal performance of double receiver compound parabolic bolic concentrator.	• A characterization of geometry and optical model was developed. • The efficiency of a static symmetrical CPC has been determined for uses of thermal appliances. • The invistigation of effects of the the receiver size on optical efficiency of CPC. • The benifits of using double receiver in one concentrator has been cleared.
A. Rabl, J. O'gallagher, R.Winston	Solar Energy	Design and test of non-evaculated solar collectors with Compound Parabolic Concentrator.	•From this paper I summarizes more than 3 year of research on non-evacuated tube and measured data of performance and critical design. • Concentrations in the upper limit of the practical range can provide better efficiency (40-50 percent) in the 100-160°C temperature range with relatively seperate tilt angle adjustments (12-20 times per year). • The design problems for non-evacuated CPC are totally different from the evacuated CPC collectors who have evacuated receivers. • Loss of heat over the reflector can become critical, since ideal CPC demands that the reflector extend all the way to the absorber.

Table 2.1: Papers for References

Chapter 3

Computational Fluid Dynamics Analysis of CPC

3.1 CPC Geometry Model Description

Numerical model of Compound Parabolic Concentrator (CPC) collector for various absorber temperatures and tilt angles using CREO software, then the geometry is imported in ANSYS software for further analysis. It has been founded steady calculations are not sufficient for simulations so that transient simulations in 3D are required for a reproduction in detail of the natural convection currents.

The size of the hot absorber surface is reduced by concentrating the incident light In the CPC collectors, but one remains at low levels of concentration (C) so that the resulting angular acceptance $\sin(\vartheta a)=1/C$ is large and tracking of the collector is not required (ϑa =20) for(C=3). For Concentration ratio (C) is 2, resulting angular acceptance $\sin(\vartheta a)=1/C$ is 2. so (ϑa =30) for(C=2). For Concentration ratio (C) is 1, resulting angular acceptance $\sin(\vartheta a)=1/C$ is 1, so (ϑa =90) for(C=1).

3.1.1 Numerical model of CPC

1. For Concentration ratio 1

In CPC collectors the size of the hot absorber surface is reduced by concentrating the incident light, but one remains at low levels of concentration C so that the resulting angular (acceptance angle) $\sin(\vartheta a)=1/C$ is large and tracking of the collector is not required ($\vartheta a \approx 90$) for($C \approx 1$).

2. For Concentration ratio 2

In CPC collectors the size of the hot absorber surface is reduced by concentrating the incident light, but one remains at low levels of concentration C so that the resulting angular (acceptance angle) $\sin(\vartheta a)=1/C$ is large and tracking of the collector is not required ($\vartheta a \approx 30$) for($C \approx 2$).

3. For Concentration ratio 3

In CPC collectors the size of the hot absorber surface is reduced by concentrating the incident light, but one remains at low levels of concentration C so that the resulting angular (acceptance angle) $\sin(\vartheta a)=1/C$ is large and tracking of the collector is not required ($\vartheta a \approx 20$) for($C \approx 3$).

Now the optical design of a CPC collector is straight forward using calculation methods of non-imaging optics (see for example Winston and Min˜ano, 2005) and standard ray tracing techniques. Because efficiency of the collector is determined by the solar gains and the thermal losses, detailed analysis of heat transfer by conduction, convection and radiation must complement the optical design. Calculations of convective heat transfer are usually based on empirical Nusselt number correlations, which are only available for the simple geometries. Their application to CPCs is limited and can be spoofing (as shown by Singh and Eames, 2011).

For the accurate prediction of the convective heat transfer numerical simulations must be used. Due to the complex geometry of the collector, same applies for the radiative heat transfer. To validate numerical simulations must always go with the experiments results.

The shape of the concentrator in CPC can be symmetric or asymmetric which can be fitted with the receiver of different configurations such as flat, wedge, tubular, and bifacial. The type and shape of the tube may influence the overall performance of the collector. Heat pipe has been found to be effective in transferring the heat gain from the evaporator to the condenser sections where it is transferred to the cooling fluid [8]. Also certain factors need to be considered in designing solar thermal CPC concentrator such as the height, aperture width and the concentration ratio.

3.2 Computational Procedure in FLUENT ANSYS (Mesh generation)

3.2.1 Setup for Simulation Analysis

The 3D CFD geometry is identical to the cross-section of the CREO sketch only the aluminum frame has been omitted. Special care was taken to precisely model the mirror. So, the shape of the mirror was modernized to the true geometry got from an image of the assembly Fig3.1. The mesh consists of one fluid zone (air) in the cavity among mirror and glass cover, all other domains are modelled same as solids. As long as in the experiment the water in the absorber was at constant temperatures, we did not include the fluid in absorber tube in our simulations.

The 3D meshes were generated only using quads, which is favorable for the accuracy of simulations. Several factors trace the resolution of the mesh. First of all there are two areas which deserve cautious meshing with high resolution: the space between a tube and

an involute of the mirror at the bottom of the CPC, where strong gradients in temperature and velocity occur Fig3.1 , and the contact surface of mirror with the top glass cover. Then, it is important that the mesh resolves the boundary layer (y $\leq$ 1condition) of the air inside the cavity close to the walls of mirror, glass and absorber. At last, the mirror and the tube are comparatively thin and must be meshed with low aspect ratio cells, which determines cell size and aspect ratio in the vicinity of these domains. The total number of cells in the mesh is the result of all the above conditions.

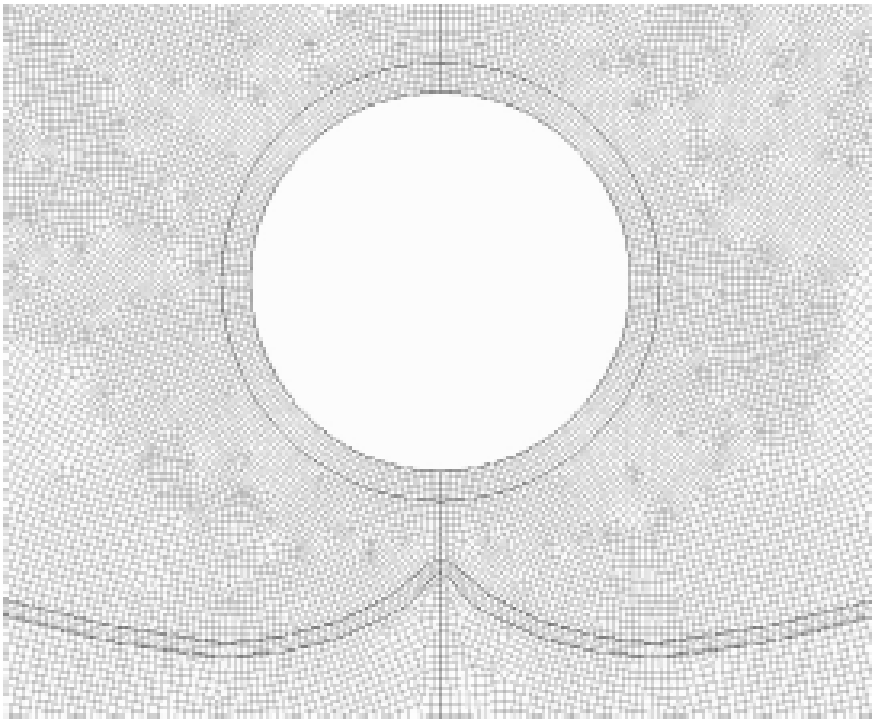

Figure 3.1: Detail of mesh 3D-A showing the area around the absorber tube

The mesh has a resolution of five cells in the tube wall and three cells in the mirror wall. The black lines show the geometric boundaries between tube, air, mirror and insulation.[8]

The finest mesh is defined by resolving the tube thickness with five and mirror thickness with three cells. The tube and mirror circumference resolution is set to 240 and 600 cells; 10 cells have been placed at shortest distance between the tube and the mirror Fig3.1

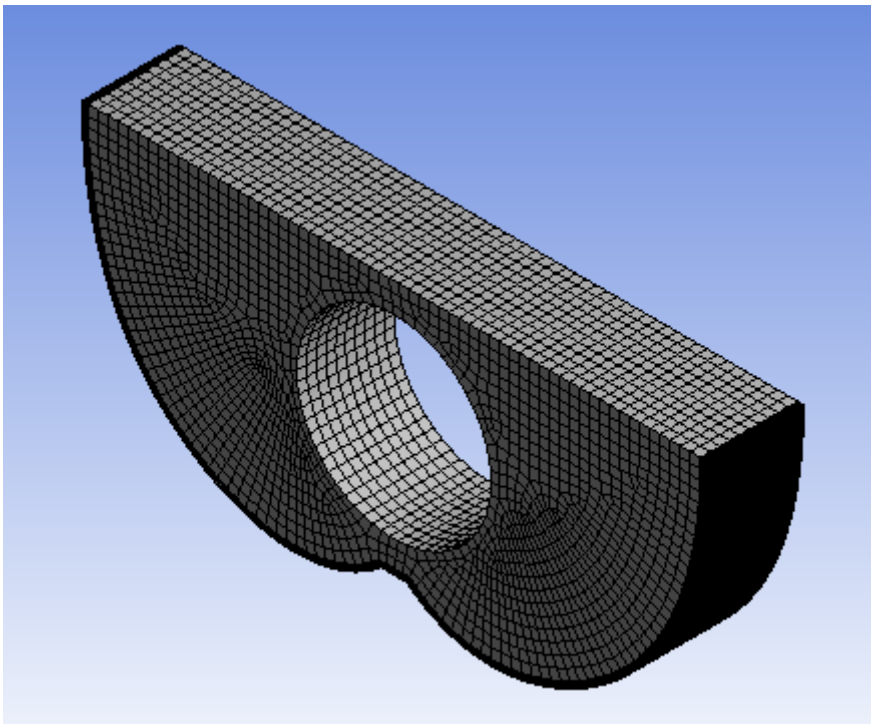

Figure 3.2: Meshing of geometry (CR-1)

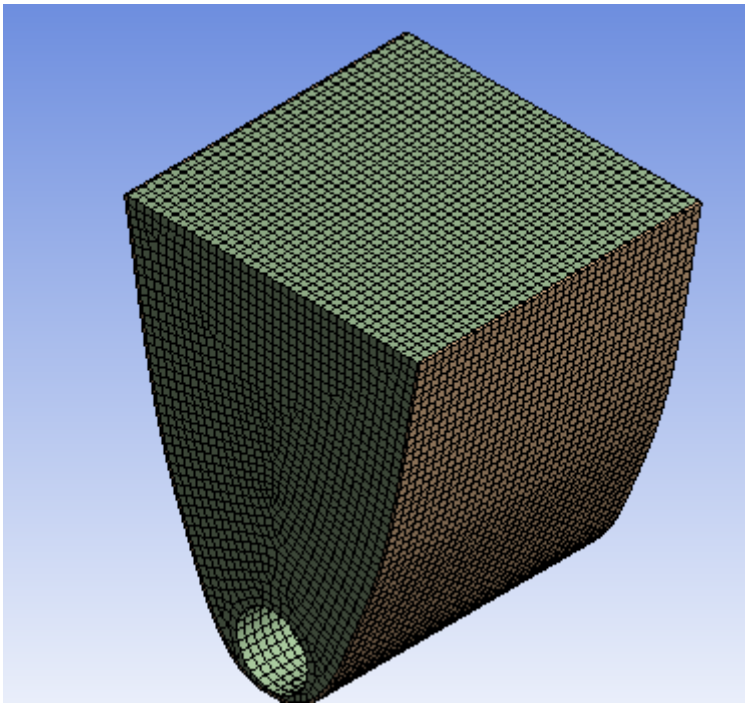

Figure 3.3: Meshing of geometry (CR-2)

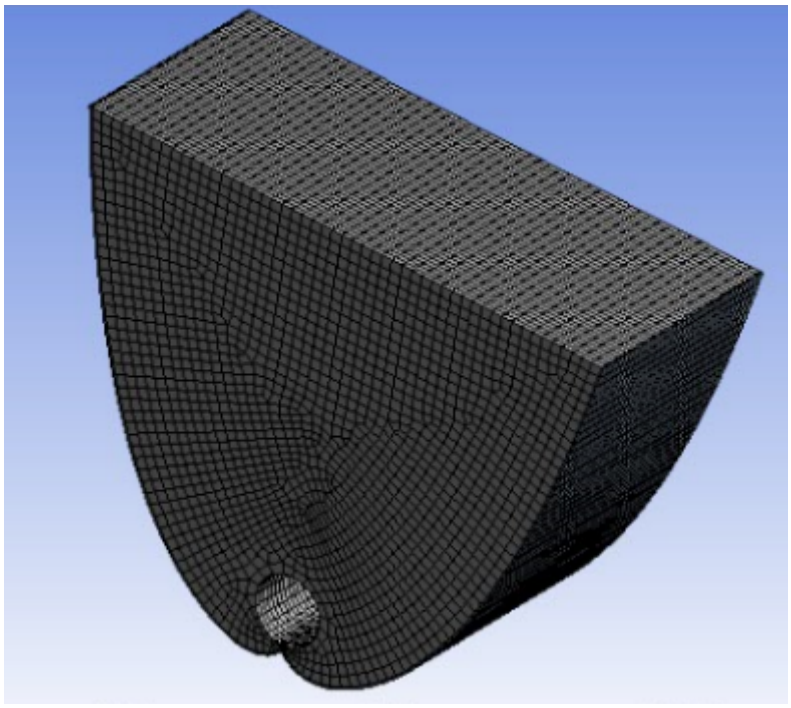

Figure 3.4: Meshing of Geometry (CR-3)

3.2.2 Mesh Report of Geometry

Table 3.1: Mesh report of geometry

	Nodes	Elements
CR-1	119632	89598
CR-2	524880	77280
CR-3	817530	633402

3.2.3 Solution Method of CPC

Calculations are performed using the Naiver– Stokes solver ANSYS in its pressure-based steady and transient formulation. Pressure velocity coupling will be realized using the COUPLED scheme with spatial discretization of second order upwind for momentum and energy. Gravitational forces and body force weighted pressure calculations will be used. For simulations with different tilt angles the mesh will be rotated accordingly.

Internal radiation exchange inside the cavity between glass, mirror and absorber will be modelled using a surface- two-surface (S2S) implementation. It is important to note, that the convergence criterion for the S2S model in ANSYS Fluent had to be as low as $10^{-}7$ to reduce the error in the radiation energy balance to acceptably low values.

We will test several turbulence models and will be founded that for our high resolution meshes the choice of the turbulence model was not critically important. All results will be calculated using the standard k–€ model, which includes the buoyancy effects in the k-

and € equations. The viscosity affected near-wall region will completely resolved all the way down to the viscous sublayer using enhanced wall treatment. This will be achieved by smoothly blending the logarithmic layer formulation with laminar formulation.

Steady 3D calculations will be allowed to converge using 600 iterations, reaching a continuum residuum of below 1/100. The residua for velocity components and energy will be lower by a factor of 100. The continuity equation could not be brought to convergence in 3D-steady calculations, because flow instabilities and turbulence prohibit a reduction of the residua to less than 0.1.

Transient calculations have been performed due to second order implicit time discretization schemes and a time-step size of 10 ms to reach sufficiently low continuity equation residua (less than 1/100).

Heat fluxes can be extracted out of 3D-transient calculations, if small local deviations will be accepted. Short calculation times for the efficient 3D simulations allowed us to simulate a diversity of scenarios. The operating pressure at a reference point in the cavity will be varied from ambient pressure down to 1 mbar. Due to the incompressible ideal gas law, the changes in operating pressure straightly influence the density of the gas in simulations.

3.3 Boundry conditions for CFD simulation of CPC

3.3.1 Boundary Conditions in CFD analysis for Concentration Ratio 1:

Figure 3.5: Boundary Condition for CR-1

Domain	Boundaries	
fluid_domain	**Boundary - contact_region src**	
	Type	INTERFACE
	Boundary - inlet_body	
	Type	WALL
	Boundary - outlet_body	
	Type	WALL
	Boundary - sunrays_face	
	Type	WALL
	Boundary - tube_surface	
	Type	WALL
outer_surface	**Boundary - reflectivity_surface contact_region trg**	
	Type	INTERFACE
	Boundary - wall outer_surface	
	Type	WALL

3.3.2 Boundary Conditions in CFD analysis for Concentration Ratio 2:

Figure 3.6: Boundary Conditions for CR-2

Domain	Boundaries	
fluid_domain	**Boundary - contact_region src**	
	Type	INTERFACE
	Boundary - inlet_body	
	Type	WALL
	Boundary - outlet_body	
	Type	WALL
	Boundary - sunrays_face	
	Type	WALL
	Boundary - tube_surface	
	Type	WALL
outer_surface	**Boundary - reflectivity_surface contact_region trg**	
	Type	INTERFACE
	Boundary - wall outer_surface	
	Type	WALL

3.3.3 Boundary Conditions in CFD analysis for Concentration Ratio 3:

Figure 3.7: Boundary Condition for CR-3

Domain	Boundaries	
fluid_domain	**Boundary - contact_region src**	
	Type	INTERFACE
	Boundary - inlet_body	
	Type	WALL
	Boundary - outlet_body	
	Type	WALL
	Boundary - sunrays_face	
	Type	WALL
	Boundary - tube_surface	
	Type	WALL
outer_surface	**Boundary - reflectivity_surface contact_region trg**	
	Type	INTERFACE
	Boundary - wall outer_surface	
	Type	WALL

3.4 Governing Equations used in simulation

3.4.1 Mass conservation (Countinuity) Equation:

$$\frac{\partial u_i}{\partial x_i}=0 \tag{3.1}$$

3.4.2 Momentum Conservation Equation:

$$\rho^{'}(\frac{\partial u_i}{\partial t}+\frac{\partial u_i u_j}{\partial x_i})=-\frac{\partial p}{\partial x_i}+\frac{\partial p}{\partial x_i}+\mu(\frac{1}{3}\frac{\partial^2 u_j}{\partial x_i x_j}+\frac{\partial^2 u_i}{\partial x_i x_j})+(\rho-\rho^{'})g \tag{3.2}$$

3.4.3 Energy Conservation Equation:

$$\rho^{'}(\frac{\partial h_{tot}}{\partial t} + \frac{\partial h_{tot} u_i}{\partial x_i}) - \frac{\partial p}{\partial t} = k\frac{\partial T}{\partial x_i x_j} \tag{3.3}$$

where $\rho^{'}$ is a reference density and $h_{tot} = h + \frac{1}{2}\|u\|^2$ is the total enthalpy.

3.4.4 Radiation Equation

$Q = \sigma\ (T_{hot}^4 - T_{cold}^4)\, A$

where σ is Stefan- Boltzmann Constant

Q is heat source

A is Surface area

T is Temperature

Chapter 4

Results and Discussion

The results obtained by CFD analysis of the CPC considering variation in concentration ratio (CR) for various considerations of surface charactristics are presented in this chapter.

4.1 Temperature distribution in CPC for CR-1

The temperature variation within the CPC for CR=1 are tabulated in table 4.1 considering variation in emissivity for tube and the reflecting surface.

Table 4.1: Results of CR-1

Sr. No	Emissivity		Time	Mean temperature of fluid at middle plane	Average temperature of tube surface
	Tube	Reflecting surface			
1	0.7	0.1	60 sec	397 K	379 K
2	0.7	0.2	60 sec	380 K	359 K
3	0.7	0.3	60 sec	373 K	339 K
4	0.9	0.1	60 sec	367 K	389 K
5	0.9	0.2	60 sec	345 K	385 K
6	0.9	0.3	60 sec	312 K	371 K
7	0.5	0.1	60 sec	418 K	360 K
8	0.5	0.2	60 sec	412 K	340 K
9	0.5	0.3	60 sec	398 K	331 K

The maximum fluid temperature distribution obtained for CR=1 (at the middle plane) , tube surface emissivity=0.5 and reflecting surface emissivity=0.1 is shown in fig 4.1

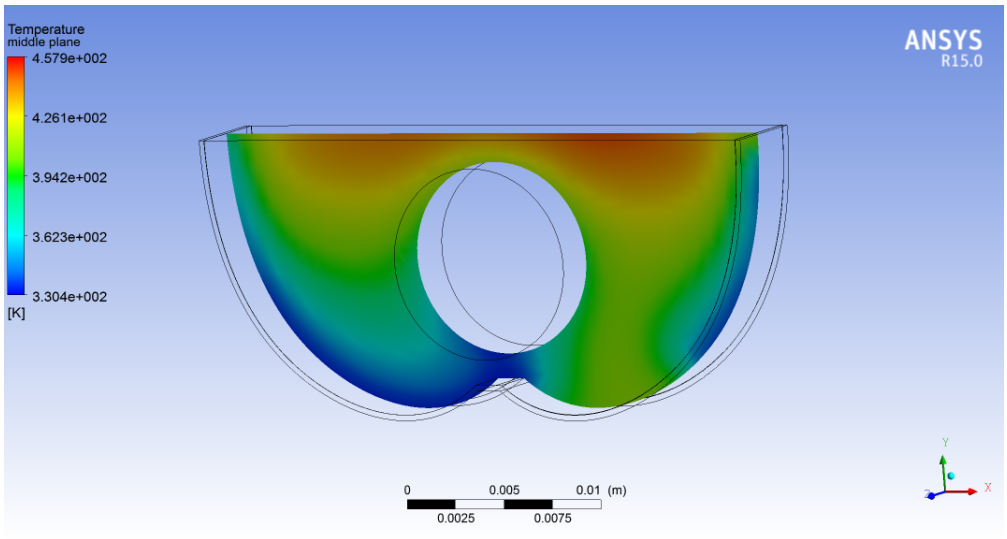

Figure 4.1: CR-1 : Maximum mean Temperature at middle plane

The maximum tube surface temperature distribution obtained for CR=1, tube surface emissivity = 0.9 and reflecting surface emissivity = 0.1 is shown in fig 4.2

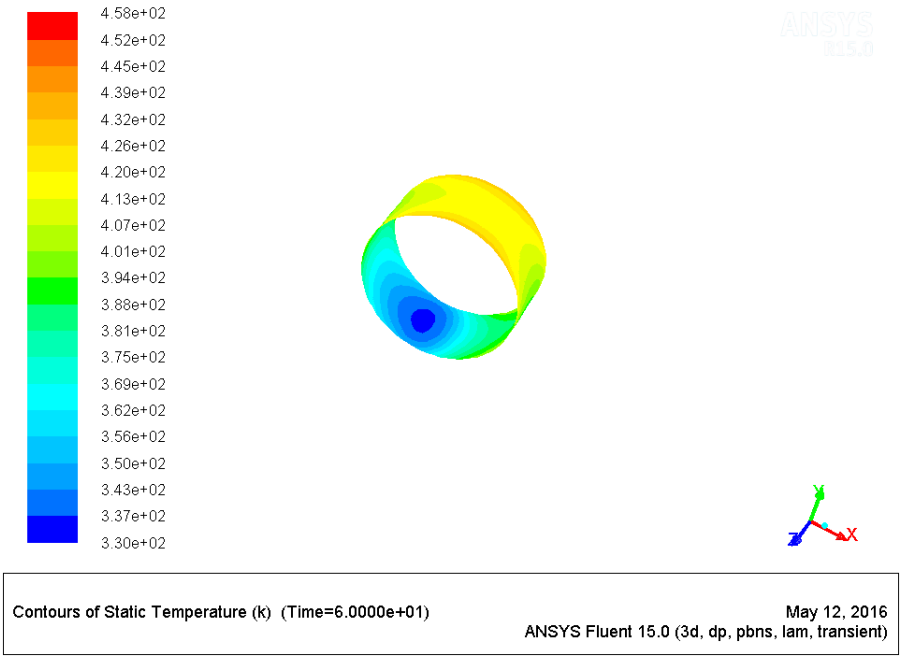

Figure 4.2: CR-1 :Temperature of tube surface

4.2 Temperature distribution in CPC for CR-2

The temperature variation within the CPC for CR=2 are tabulated in table 4.2 considering variation in emissivity for tube and the reflecting surface.

Table 4.2: Results of CR-2

Sr. No	Emissivity		Time	Mean temperature of fluid at middle plane	Average temperature of tube surface
	Tube	Reflecting surface			
	0.7	0.1	60 Sec	350 K	338.5 K
	0.7	0.2	60 Sec	335 K	318.5 K
	0.7	0.3	60 Sec	331 K	317 K
	0.9	0.1	60 Sec	345 K	342 K
	0.9	0.2	60 Sec	340 K	332 K
	0.9	0.3	60 Sec	335 K	328 K
	0.5	0.1	60 Sec	380 K	316 K
	0.5	0.2	60 Sec	368 K	315 K
	0.5	0.3	60 Sec	367 K	310 K

The maximum fluid temperature distribution obtained for CR=2 (at the middle plane) , tube surface emissivity=0.5 and reflecting surface emissivity=0.1 is shown in fig 4.3

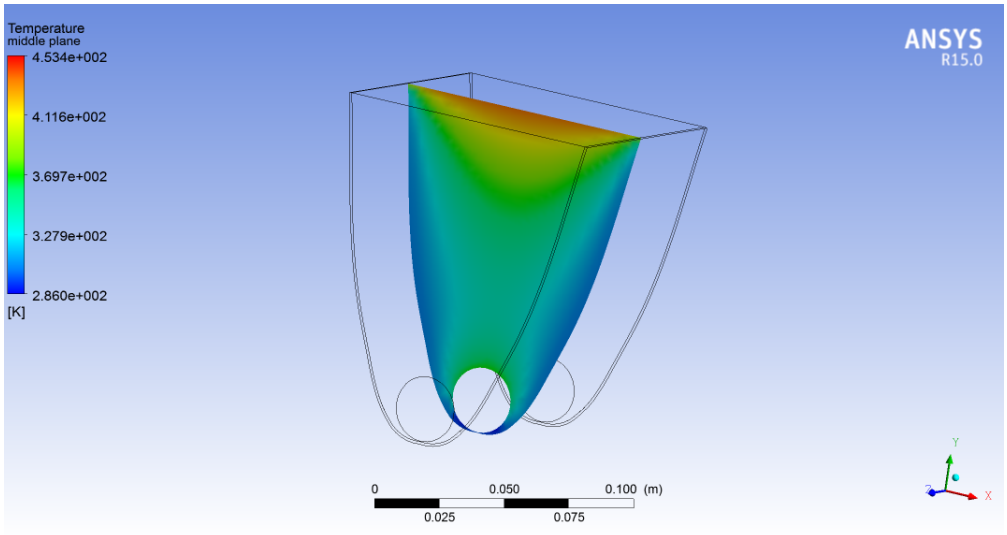

Figure 4.3: CR-2: Maximum mean Temperature at middle plane

The maximum tube surface temperature distribution obtained for CR=2, tube surface emissivity = 0.9 and reflecting surface emissivity = 0.1 is shown in fig 4.4

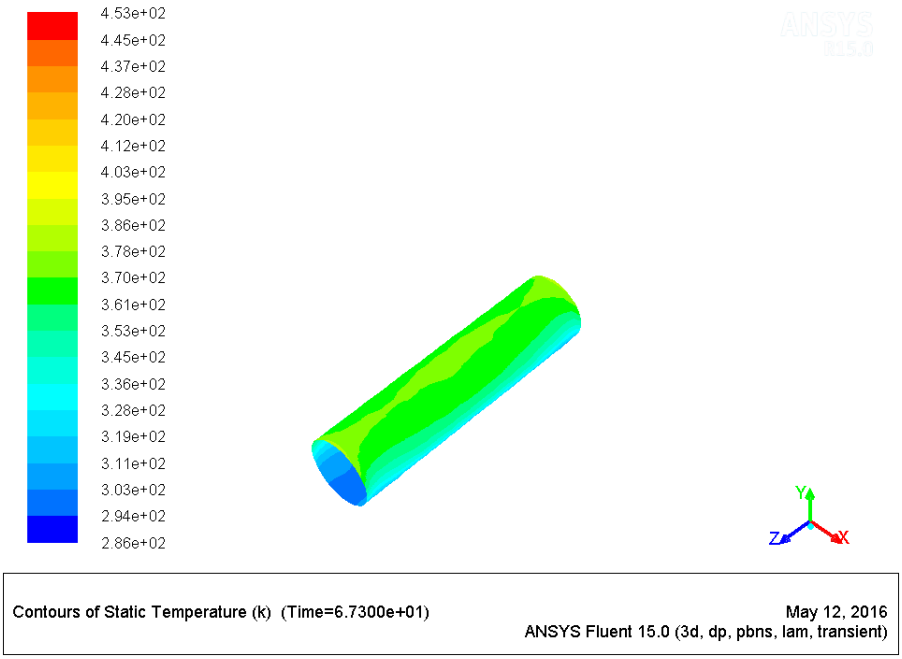

Figure 4.4: CR-2: Temperature of tube surface

4.3 Temperature distribution in CPC for CR=3

The temperature variation within the CPC for CR=3 are tabulated in table 4.3 considering variation in emissivity for tube and the reflecting surface.

Table 4.3: Results of CR-3

Sr. No	Emissivity		Time	Mean temperature of fluid at middle plane	Average temperature of tube surface
	Tube	Reflecting surface			
	0.7	0.1	60 sec	480 K	356.27 K
	0.7	0.2	60 sec	475 K	353 K
	0.7	0.3	60 sec	474 K	350.7 K
	0.9	0.1	60 sec	470 K	393.2 K
	0.9	0.2	60 sec	465 K	392K
	0.9	0.3	60 sec	462 K	391 K
	0.5	0.1	60 sec	510 K	347.5 K
	0.5	0.2	60 sec	508 K	344 K
	0.5	0.3	60 sec	507 K	343 K

The maximum fluid temperature distribution obtained for CR=3 (at the middle plane) , tube surface emissivity=0.5 and reflecting surface emissivity=0.1 is shown in fig 4.5

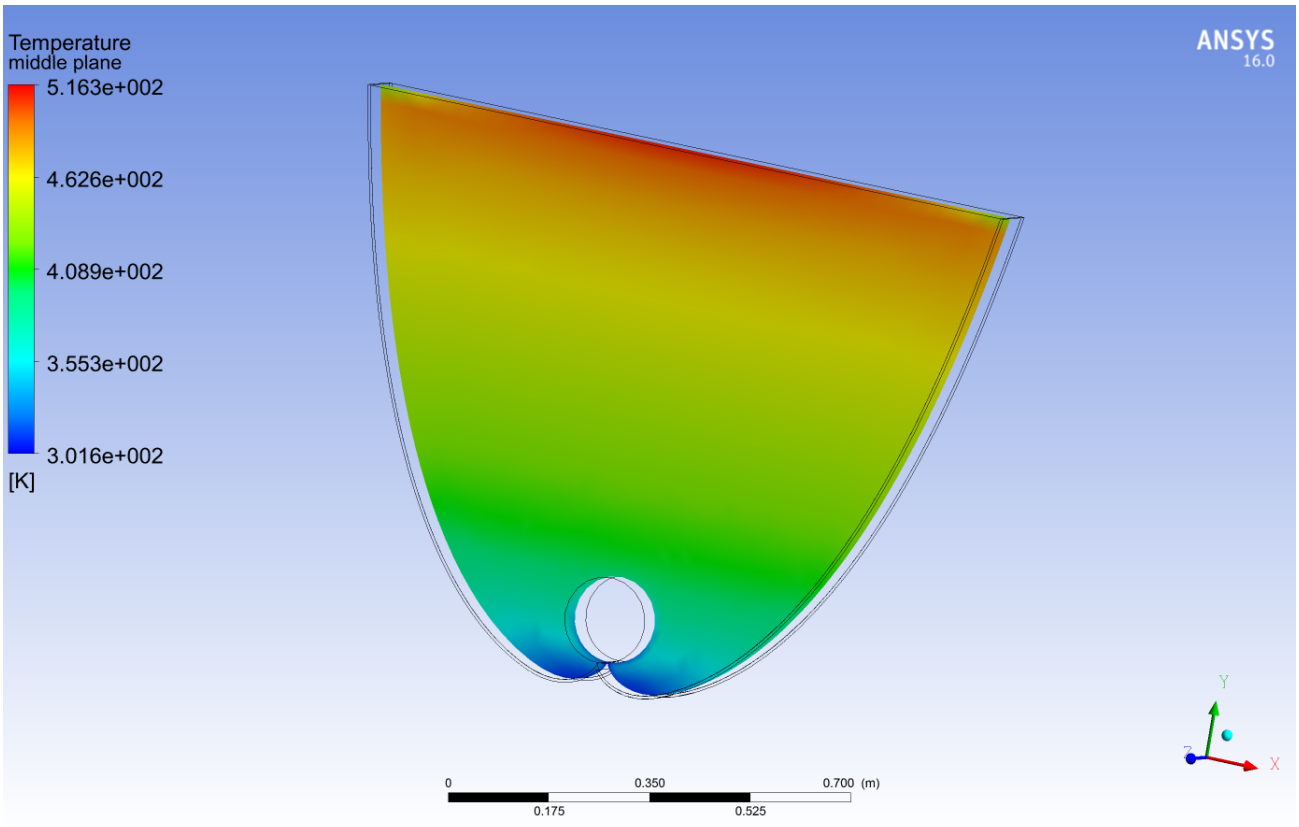

Figure 4.5: CR-3 :Maximum mean Temperature at middle plane

The maximum tube surface temperature distribution obtained for CR=3, tube surface emissivity = 0.9 and reflecting surface emissivity = 0.1 is shown in fig 4.6

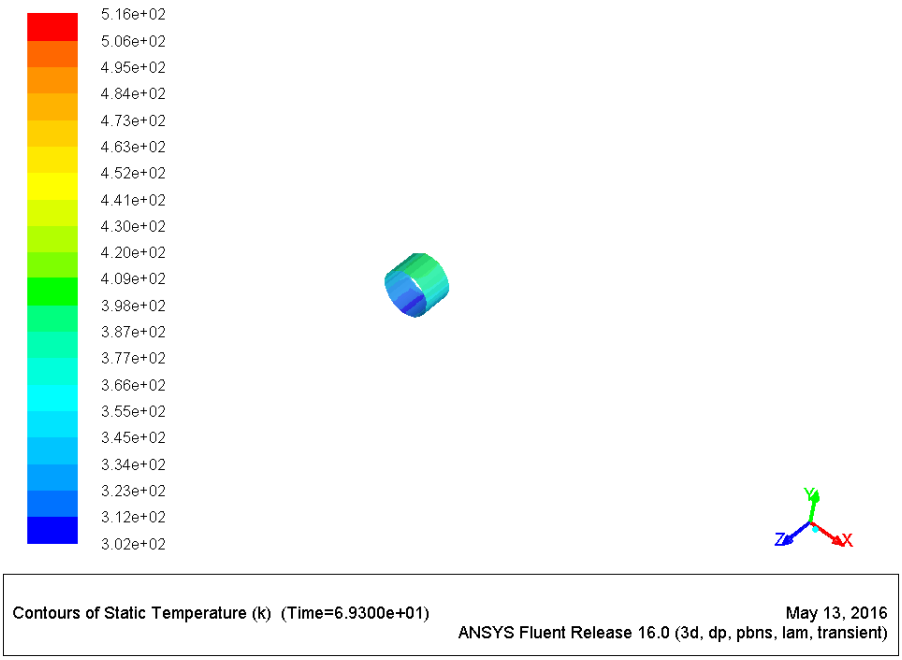

Figure 4.6: CR-3:Temperature of tube surface

4.4 Discussion

The CFD analysis of the CPC for various Concentration ratio (CR) and surface characteristics reveal the tube surface temperature and the air temperature profile. The results are tabulated in Table 4.1, 4.2, and 4.3. The temperature profiles are shown in Fig. 4.1 - 4.6 .

The analysis of results reveal the relative influence of Concentration ratio on the temperature profiles within the CPC.

From the CFD results obtained for various Concentration Ratio (CR) and surface radiation characteristics, it can be observed that there are typical circulating flow pattern of the natural convection within the CPC. The effect of a larger CR on the temperature.

The avarage temperature of tube surface for various CR(CR-1, CR-2, CR-3) and surface characteristics are shown in table 4.4 . Further more The mean fluid temperature at middle plane for various CR and surface characteristics are shown in table 4.5 .

Table 4.4: The avarage temperature of tube surface for various CR and surface characteristics

Sr No.	Emissivity		Time	Average Temperature of tube surface		
	Tube	Reflecting Surface		CR-1	CR-2	CR-3
1	0.7	0.1	60 sec	379.5 K	338.5	356.2 K
2	0.7	0.2	60 sec	359 K	318 K	353 K
3	0.7	0.3	60 sec	339 K	317 K	350.7 K
4	0.9	0.1	60 sec	389 K	342 K	393.2 K
5	0.9	0.2	60 sec	385 K	332 K	392 K
6	0.9	0.3	60 sec	371 K	328 K	391 K
7	0.5	0.1	60 sec	360 K	316 K	347.5 K
8	0.5	0.2	60 sec	340 K	315 K	344 K
9	0.5	0.3	60 sec	331 K	310 K	343 K

The analysis of data from Table 4.4 points to the higher temperature of the tube surface for CR 3. Also for the value of tube surface emissivity of 0.9 and reflecting surface emissivity of 0.1, the result of tube surface temperature is obtained to be higher. This is due to a larger proportion of radiation accepted at CR 3 as well as due to a larger reflectivity of reflecting surface and improved absorption at tubular surface.

Table 4.5: The mean fluid temperature at middle plane for various CR and surface characteristics

Sr. No.	Emissivity		Time	Mean Temperature of fluid at middle plane		
	Tube	Reflecting surface		CR-1	CR-2	CR-3
1	0.7	0.1	60 sec	397 K	350 K	480 K
2	0.7	0.2	60 sec	380 K	335 K	475 K
3	0.7	0.3	60 sec	373 K	331 K	474 K
4	0.5	0.1	60 sec	418 K	380 K	510 K
5	0.5	0.2	60 sec	412 K	368 K	508 K
6	0.5	0.3	60 sec	398 K	367 K	507 K
7	0.9	0.1	60 sec	367 K	345 K	470 K
8	0.9	0.2	60 sec	345 K	340 K	465 K
9	0.9	0.3	60 sec	312 K	335 K	462 K

The analysis of fluid temperature in table 4.5 reveal that for CR 3, the value of tube surface emissivity of 0.5 and reflecting surface emissivity of 0.1, the fluid temperature is higher. This is due to larger preportion of energy reflected from the tube which leads to a higher temperature of fluid.

After Performing the CFD Analysis the following results are obtained.

• maximum mean temperature of Fluid at the middle Plane in following condition:

Concentration ratio 3

Emissivity on tube surface 0.5

Emissivity on Reflecting surface 0.1

Reflectivity on tube surface 0.5

Reflectivity on Reflecting surface 0.9

• Maximum Average Temperature of Tube Surface in Following Condition

Concentration ratio 3

Emissivity on tube surface 0.9

Emissivity on Reflecting Surface 0.1

Reflectivity on tube surface 0.1

Reflectivity on Reflecting surface 0.9

Chapter 5

Conclusion and Future Work

The following are the conclusions:

- The geometric model of the CPC was prepared using CREO software
- The meshing of the geometry prepared was completed using ANSYS.
- The CFD analysis of the CPC was performed. (CR of 1,2 and 3)
- The influence of change of Concentration Ratio and surface radiation properties of the collector surface on the temperature distribution within the CPC was studied

- The CFD analysis considering different concentration ratio and surface properties (radiation related) reveal that the highest tube surface temperature are obtained for a concentration ratio of 3 with tube surface emissivity of 0.9 and reflector surface reflectivity of 0.9.

- The CFD analysis considering different concentration ratio and surface properties (radiation related) reveal that the highest fluid temperature are obtained for a concentration ratio of 3 with tube surface emissivity of 0.5 and reflector surface reflectivity of 0.9.

The following are the future studies that can be undertaken:

1. The numerical results may be validated with experimental studies.

2. The numerical simulation may be undertaken considering actual absorber/collector tubes

3. The effect of variation of solar radiation input on the CPC performance may be studied.

Bibliography

[1] Rabl, "*Solar Concentrators with Maximal Concentration for Cylindrical Absorbers*", Applied Optics, vol. 15, No: 7, pp.1871-1873, 1976.

[2] Rabl A. Optical and thermal properties of compound parabolic concentrator. Solar Energy; 18:497–511, 1976.

[3] Rabl A. Active Solar Collector and Their Applications, 1st edn. Oxford University Press: New York, 147–169, 1985.

[4] W. Lipinski and A. Steinfeld, "*Annular Compound Parabolic Concentrator*", Journal of Solar Energy Engineering, Vol.128, pp. 121-124, 2006.

[5] S. P. and J.K. Nayak, Solar energy principle of thermal collection and storage, Tata Mc Graw Hill, Third Edition, Page no 233,234, 2008

[6] Winston, R., Minlano, J.C., 2005. Non imaging Optics. Elsevier Academic Press. Singh, H., Eames, P.C., 2011.

[7] A review of natural convection heat transfer correlations in rectangular cross-section cavities and their potential applications of compound parabolic concentrating (CPC) solar collector cavities. Applied Thermal Engineering 31, 2186–2196.

[8] Ch. Reichl, F. Hengstberger, Ch. Zauner. Heat transfer mechanisms in a compound parabolic concentrator: Comparison of computational fluid dynamics simulations to particle image velocimetry and local temperature measurements.

[9] A.A. Hachicha, I. Rodríguez 1, R. Capdevila, A. Oliva Heat transfer analysis and numerical simulation of a parabolic trough solar collector. Centre Tecnològic de Transferència de Calor, Universitat Politècnica de Catalunya, ETSEIAT, Colom 11, 08222 Terrassa, Barcelona, Spain. 1993

[10] Centre Tecnològic de Transferència de Calor, Universitat Politècnica de Catalunya, ETSEIAT, Colom 11, 08222 Terrassa, Barcelona, Spain. On the CFD&HT of the flow around a parabolic trough solar collector under real working conditions.1993

[11] B. Abdullahi , R.K. AL-Dadah, S. Mahmoud, R. Hood. Optical and thermal performance of double receiver compound parabolic concentrator, Volume 159 ,December 2015, Pages 1-10

[12] J. A. Duffie and W. A. Beckman, Solar Engineering of Thermal Processes. Wiley, New York (1980).

[13] B S Mangal , Solar Power Engineering, Tata Mc Graw hill, 1993.